lattice, and if

$$L_b = L_m \tag{2}$$

then

$$f_\infty = \frac{1}{2\pi}\sqrt{\left(\frac{1}{C_1(L_1 + L_m)}\right)} \tag{3}$$

from which the motional capacitance C_1 may be calculated.

Considering the lowpass and bandpass components of the network, we obtain their respective loads as follows:

$$R_{LP} = \sqrt{\left(\frac{L_b}{2C_0}\right)} \tag{4a}$$

and

$$R_{BP} = \frac{2\pi\Delta f L_1}{q} \qquad q = 1.414 \tag{4b}$$

Making the load resistances the bandstop filter load, we obtain the static capacitance

$$C_0 = \frac{1}{4\pi^2 \Delta f f_\infty L_1} \tag{5}$$

A similar bandstop MCF filter having a lowpass response outside the stopband could also be obtained by direct synthesis such as from the original even-degree elliptic function,[2] or by transformation of the even-degree elliptic function highpass prototypes.[3]

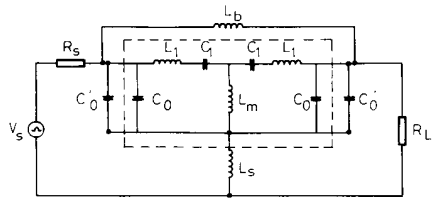

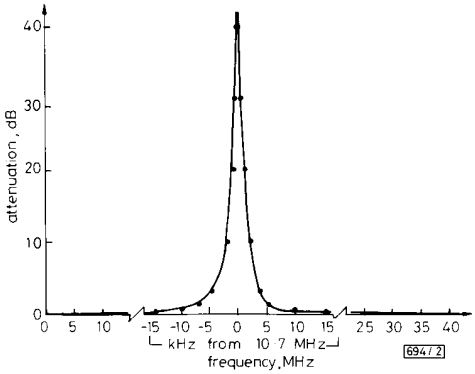

Fig. 2 *Computer and measured responses of bandstop monolithic crystal filter*

$L_1 = 32{\cdot}00\,\text{mH}$
$L_m = 25{\cdot}36\,\mu\text{H}$
$L_b = 25{\cdot}36\,\mu\text{H}$
$L_s = 6.34\,\mu\text{H}$
$C_1 = 6{\cdot}90790283 \times 10^{-3}\,\text{pF}$
$C_0' + C_0 = 8{\cdot}724\,\text{pF}$
$R_s = 1205\,\Omega$
$R_L = 1205\,\Omega$
$Q_{crystal} = 20000$
$Q_{coil} = 100$
——— computed
● measured

We now consider the bandstop MCF filter having an allpass response outside the stopband by adding a series inductance L_S. Its value may easily be found by noting that the load for the highpass component is

$$R_{HP} = \sqrt{\left(\frac{2L_s}{C_0}\right)} \tag{6}$$

and on comparing with eqn. 4*a* we obtain

$$L_s = \frac{L_b}{4} \tag{7}$$

The inclusion of L_s and the practical Q factors for the crystal and inductors will cause a widening of the 3 dB bandwidth and shift down the notch frequency. To compensate for the changes, we use a smaller Δf and slightly offset f_∞. An example to illustrate the design is given in Fig. 2 for a bandstop MCF filter having a notch frequency at 10.7 MHz and a 10 kHz bandwidth, using the data $f_\infty = 10{\cdot}7004$ MHz and $\Delta f = 8.48$ kHz. A comparison for the computed and measured responses is also given for a crystal Q of 20 000 and inductor Q of 100.

Acknowledgment: The author wishes to thank Hy-Q International (Singapore) for its facility in making the bandstop monolithic crystal filter.

S. K. S. LU

Department of Electrical Engineering
University of Malaya
Kuala Lumpar
Malaysia

29th April 1991

References

1 SIMPSON, H. A. *et al.*: 'Composite filter structures incorporating monolithic crystal filter and LC networks'. Proc. 25th Ann. Symp. Frequency Control, 1971, pp. 287–296
2 LU, S. K. S.: 'Even-degree elliptic function monolithic crystal filters', *IEE J. Electron. Circuits & Syst.*, 1978, **2**, (5), pp. 143–146
3 LU, S. K. S.: 'Tables of even-degree elliptic function highpass prototypes'. Available on request from the author

SELECTIVITY-IMPROVED *E*-PLANE FILTER FOR MILLIMETRE-WAVE APPLICATIONS

Indexing terms: Microwave filters, Filters, Microwave devices

Measurements on a Ka-band selectivity-improved *E*-plane filter prototype are compared with computed predictions and are found to be in excellent agreement. The measured insertion loss is 1·5 dB, and the bandwidth is 180 MHz centred at 32·8 GHz. These prototype measurements confirm that this design has the potential for significantly improving the performance of filter components in the millimetre-wave frequency range.

Introduction: To improve the skirt selectivity of standard millimetre-wave all-metal insert *E*-plane filters[1–3] and simultaneously maintain compatibility with the millimetre-wave integrated circuit manufacturing process, a new class of *E*-plane filter has been introduced in References 4–6. The design is based on inductively coupled stopband sections as additions to the conventional component (see Fig. 1), hence providing attenuation peaks in the filter response. However, measurements have only been presented at frequencies below 10 GHz and for the highly unsymmetrical filter structure,[6] which sacrifices the response in the lower stopband for the benefit of attenuation poles close to the upper band edge. The more critical design with poles close to both sides of the passband[4,5] has not yet been verified experimentally. Owing to the

extremely tight coupling between the two resonators that form one stopband stub[4] and due to their high quality factor requirements, this design has always been regarded as an uncertain candidate for millimetre-wave applications.

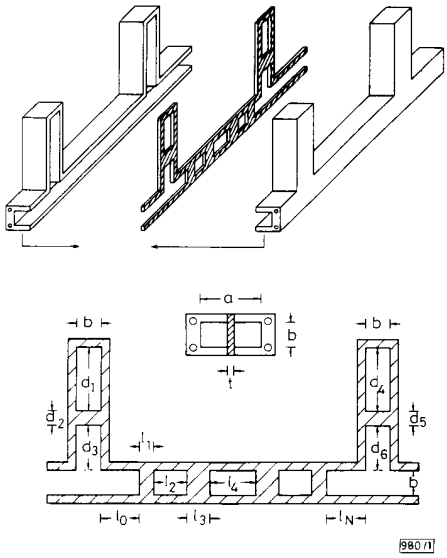

Fig. 1 *Selectivity-improved E-plane filter*

Dimensions of Ka-band prototype: $a = 7{\cdot}16$ mm, $b = 3{\cdot}52$ mm, $t = 127\,\mu$m (supplier specification), $l_0 = l_8 = 9{\cdot}14$ mm, $l_1 = l_7 = 1{\cdot}52$ mm, $l_2 = l_4 = l_6 = 4{\cdot}22$ mm, $l_3 = l_5 = 4{\cdot}85$ mm, $d_1 = d_4 = 10{\cdot}95$ mm, $d_2 = d_5 = 0{\cdot}2$ mm, $d_3 = d_6 = 7{\cdot}3$ mm

The sole purpose of this Letter is to demonstrate the realisability and applicability of this filter structure. Therefore, a comparison between theoretical results and measurements is presented for the example of a Ka-band prototype. Excellent agreement and performance are obtained, hence confirming the design procedures in References 4 and 5.

Theory and design: The selected-mode scattering matrix method used for the analysis of the selectivity-improved *E*-plane filter has already been described in Reference 4 and, in more detail, in Reference 5. Therefore, only the basic steps are presented here.

The conventional metal insert filter sections (Fig. 1, $l_1 - l_1$) are analysed by a set of TE^x_{mo} modes, whereas the *E*-plane waveguide T-junction calculation requires TE^x_{in} modes. (The TE^x_{mn} mode spectrum is described in Reference 7.) The electromagnetic field can therefore be derived from the *x*-component of the vector potential A_h.

$$\boldsymbol{E} = \nabla \times (A_{hx}\boldsymbol{e}_x) \tag{1}$$

$$\boldsymbol{H} = \frac{j}{\omega\mu} \nabla \times \nabla \times (A_{hx}\boldsymbol{e}_x) \tag{2}$$

(For details on A_{hx}, refer to eqn. 2 in Reference 4).

For the field matching at the two general discontinuities involved, the following modes are selected: $TE^x_{1,0}$ to $TE^x_{35,0}$ and $TE^x_{1,1}$ to $TE^x_{1,4}$ for the waveguide bifurcation, and $TE^x_{1,0}$ to $TE^x_{9,0}$ and $TE^x_{1,n}$ to $TE^x_{1,15}$ for the T junction.[4,5] For all *S*-matrix combining algorithms, however, only the lowest nine modes are selected: five modes of the TE^x_{mo} spectrum plus four modes of the TE^x_{in} spectrum.

The conventional *E*-plane filter and the stopband stubs are designed separately using optimisation procedures (see, for example, Reference 2). A final optimisation of the complete structure fine tunes the filter response with respect to passband return loss and ripple.

Results: Using this procedure, a three-resonator *E*-plane filter including two stopband stubs has been designed and fabricated. The initial design was for 33 GHz. Owing to extreme limitations in the manufacturing process, which mainly affected the overall waveguide width (7·16 instead of 7·112 mm), the midband frequency dropped to 32·8 GHz. With the measured dimensions, as given in the legend of Fig. 1, the filter was analysed again, and a direct comparison with measurements on a Wiltron 360 vector network analyser is given in Figs. 2 and 3. Note that the scales of ordinates differ slightly whereas the frequency ranges in each Figure are identical.

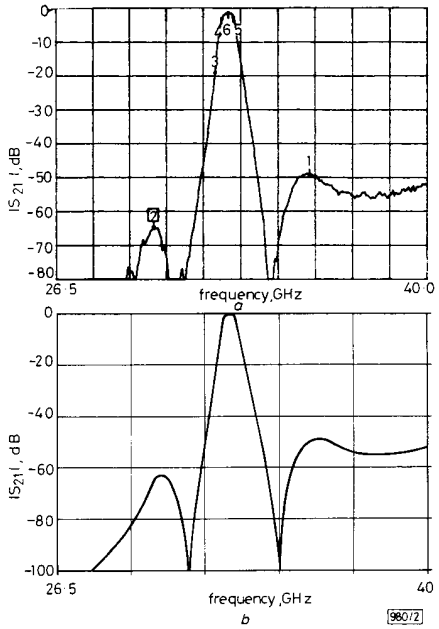

Fig. 2 *Transmission coefficient against frequency*

a Measured
b Calculated

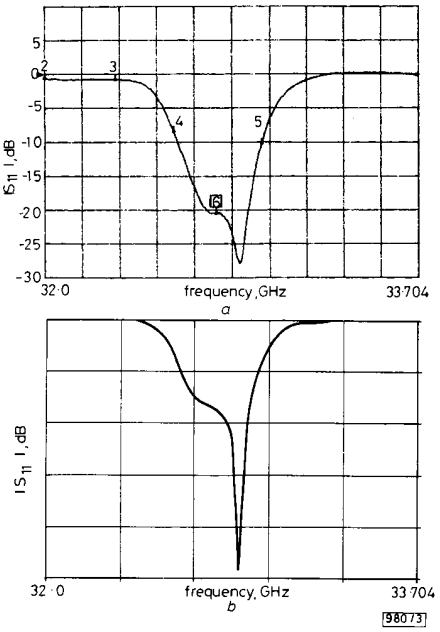

Fig. 3 *Reflection coefficient against frequency*

a Measured
b Calculated

Fig. 2 shows the measured and calculated transmission coefficients, in decibels, over the complete Ka-band frequency range. Excellent agreement is achieved with the exception of a small shift in frequency which is most likely a result of the tolerances of $\pm 10\,\mu m$ in measuring the actual circuit dimensions. This also holds for Fig. 3 where the measured reflection coefficient of $-20{\cdot}46$ dB (marker 6) is better than the calculated value $-17{\cdot}3$ dB at the same frequency. From Figs. 2 and 3, it follows that the minimum insertion loss is 1·45 dB and that the 20 dB return loss bandwidth is 180 MHz. It should be noted that the measured stopband poles are more than 80 dB down, hence indicating a sufficient quality factor for the inductively coupled stopband sections.

Fig. 4 shows a photograph of the opened Ka-band filter prototype. Note that owing to the tight coupling of the two resonators involved in one stopband section, extremely small strip widths (d_2 and d_5 in Fig. 1) have to be realised, where the minimum realisable strip width is usually of the order of the metal sheet thickness. In this design, both stopband sections produce each two identical poles immediately to the left and the right of the passband.[4] A theoretical design using different pole frequencies has been presented in Reference 5.

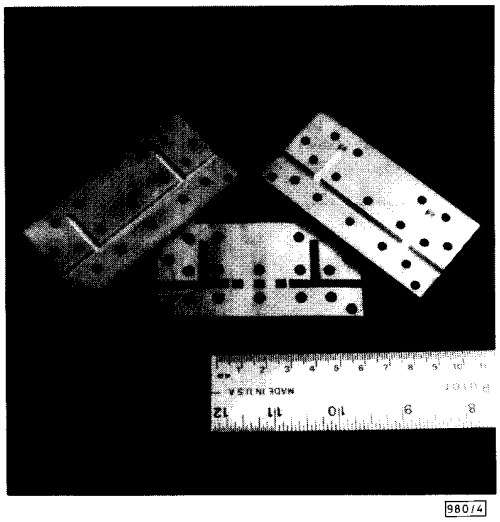

Fig. 4 *Photograph of selectivity-improved Ka-band E-plane filter prototype*

Conclusions: A comparison between theoretical and measured data of a Ka-band selectivity-improved *E*-plane filter is presented. The excellent agreement obtained confirms the selected-mode scattering matrix design method introduced either. Moreover, it proves the realisability and applicability of this type of filter structure. The characteristics of the prototype are: 1·5 dB insertion loss, a 20 dB return-loss bandwidth of 180 MHz centred at 32·8 GHz, and attenuation poles of more than 80 dB. It is expected that these measurements contribute to the pool of improved-performance filter structures for millimetre-wave applications.

J. BORNEMANN

Department of Electrical and Computer Engineering
University of Victoria
PO Box 3055
Victoria, BC V8W 3P6, Canada

7th June 1991

References

1 SHIH, Y.-C.: 'Design of waveguide E-plane filters with all-metal inserts', *IEEE Trans.*, July 1984, **MTT-32**, pp. 695–704
2 VAHLDIECK, R., BORNEMANN, J., ARNDT, F., and GRAUERHOLZ, D.: 'Optimized waveguide E-plane metal insert filters for millimeter-wave applications', *IEEE Trans.*, January 1983, **MTT-31**, pp. 65–69
3 MANSOUR, R. R., and MACPHIE, R. H.: 'An improved transmission matrix formulation of cascaded discontinuities and its application to E-plane circuits', *IEEE Trans.*, December 1986, **MTT-34**, pp. 1490–1498
4 BORNEMANN, J.: 'A new class of E-plane integrated millimetre-wave filters'. IEEE MTT-S Intl. Microwave Symp. Dig., May 1989, pp. 599–602
5 BORNEMANN, J.: 'Design of elliptic-functions-type E-plane filters for millimeter-wave applications'. Proc. MIOP '90, Stuttgart, Germany, February/March 1990, pp. 501–506
6 MANSOUR, R. R., and FOULADIAN, J.: 'Analysis and design of extracted pole E-plane filters', *Microw. and Opt. Technol. Lett.*, August 1989, **2**, pp. 286–291
7 BORNEMANN, J., and VAHLDIECK, R.: 'Characterization of a class of waveguide discontinuities using a modified TE^z_{mn} mode approach', *IEEE Trans.*, December 1990, **MTT-38**, pp. 1816–1822

FREQUENCY-HOPPED SPREAD-SPECTRUM RANDOM ACCESS WITH LOCAL ADAPTATION

Indexing terms: Data transmission, Codes and coding, Digital communication systems

A decentralised transmission policy that rejects a blocked packet that has been retransmitted a number of times is analysed for the frequency-hopping channel. For stability considerations and for channel throughput increase, the information packet is enclosed by a Reed–Solomon code. The way in which the code rate should be adjusted and the number of transmission attempt pairs that guarantees network stability are investigated.

Introduction: It is well known that random access channel sharing techniques of the ALOHA class are characterised by the bistable mechanism, in which a long term condition of low throughput and high delay may be experienced.[1] Several strategies have been designed to stabilise the random access system, such as the collision resolution algorithm,[2] where transmissions are deferred until the current conflict is solved, and the decentralised control scheme,[3] where the retransmission probability is updated according to previous channel outcomes.

The undesirable bistable behaviour occurs basically because of the unsuccessful transmission of packets (i.e. packet failures), and the rate of packet failure can be controlled either by controlling the error (erasure) correction capability of the packet or by maintaining the channel traffic below a certain level. One way to do the latter is to permanently reject a blocked packet that has been retransmitted a certain number of times. In most realistic situations a small rejection rate is tolerable, especially if the rejected packets have already been delayed too long to be important. One way to control the error (erasure) correction capability is to control the code rate (i.e. control the amount of redundancy) of the packet.

We investigate a transmission policy for the frequency-hopping (FH) channel, under which a blocked packet that has been retransmitted a certain number of times is permanently rejected. To implement this transmission policy each station only needs to know whether or not its own transmission is successful. For stability considerations and for channel throughput increase we assume that each information packet is encoded by a Reed–Solomon code. We investigate how the code rate should be adjusted in accordance with the maximum number of transmission attempts for the network to be stabilised.

Transmission policy and channel model: We assume that the number of new packets transmitted in each slot is given by a sequence of independent Poisson random variables with mean λ. If a packet is blocked the packet is retransmitted with probability p. After K unsuccessful transmissions, the packet is rejected and declared lost. By the Poisson approximation to binomial distribution, the distribution of the number of packet transmissions in slot t is approximately Poisson with mean G_t. For approximation bounds, see Reference 4.